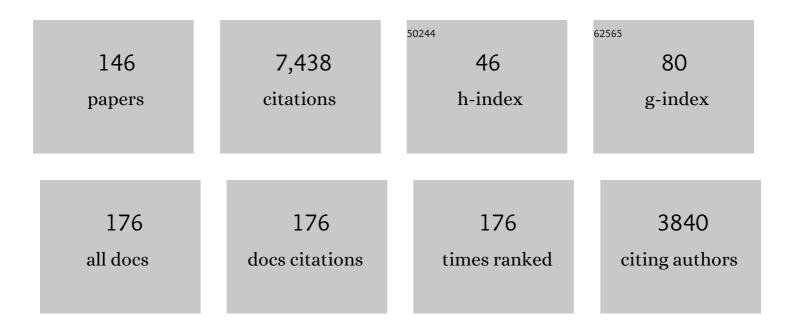
List of Publications by Year in descending order

Source: https://exaly.com/author-pdf/87940/publications.pdf Version: 2024-02-01



IÃ1/ DOEN ROALIN

#	Article	IF	CITATIONS
1	Successful treatment of active ankylosing spondylitis with the anti–tumor necrosis factor α monoclonal antibody infliximab. Arthritis and Rheumatism, 2000, 43, 1346-1352.	6.7	506
2	The impact of aging and gender on brain viscoelasticity. NeuroImage, 2009, 46, 652-657.	2.1	345
3	Noninvasive assessment of the rheological behavior of human organs using multifrequency MR elastography: a study of brain and liver viscoelasticity. Physics in Medicine and Biology, 2007, 52, 7281-7294.	1.6	295
4	Nonâ€invasive measurement of brain viscoelasticity using magnetic resonance elastography. NMR in Biomedicine, 2008, 21, 265-271.	1.6	275
5	MR-elastography reveals degradation of tissue integrity in multiple sclerosis. NeuroImage, 2010, 49, 2520-2525.	2.1	262
6	Assessment of liver viscoelasticity using multifrequency MR elastography. Magnetic Resonance in Medicine, 2008, 60, 373-379.	1.9	227
7	Brain Viscoelasticity Alteration in Chronic-Progressive Multiple Sclerosis. PLoS ONE, 2012, 7, e29888.	1.1	195
8	Structure-sensitive elastography: on the viscoelastic powerlaw behavior of in vivo human tissue in health and disease. Soft Matter, 2013, 9, 5672.	1.2	153
9	Fractional encoding of harmonic motions in MR elastography. Magnetic Resonance in Medicine, 2007, 57, 388-395.	1.9	152
10	<i>In vivo</i> viscoelastic properties of the brain in normal pressure hydrocephalus. NMR in Biomedicine, 2011, 24, 385-392.	1.6	146
11	The Influence of Physiological Aging and Atrophy on Brain Viscoelastic Properties in Humans. PLoS ONE, 2011, 6, e23451.	1.1	145
12	High-Resolution Mechanical Imaging of Glioblastoma by Multifrequency Magnetic Resonance Elastography. PLoS ONE, 2014, 9, e110588.	1.1	120
13	Quantitation of simulated short echo time1H human brain spectra by LCModel and AMARES. Magnetic Resonance in Medicine, 2004, 51, 904-912.	1.9	113
14	Tomoelastography by multifrequency wave number recovery from time-harmonic propagating shear waves. Medical Image Analysis, 2016, 30, 1-10.	7.0	111
15	In vivo waveguide elastography of white matter tracts in the human brain. Magnetic Resonance in Medicine, 2012, 68, 1410-1422.	1.9	110
16	Viscoelasticity-based MR elastography of skeletal muscle. Physics in Medicine and Biology, 2010, 55, 6445-6459.	1.6	109
17	Shear wave group velocity inversion in MR elastography of human skeletal muscle. Magnetic Resonance in Medicine, 2006, 56, 489-497.	1.9	106
18	Multifrequency inversion in magnetic resonance elastography. Physics in Medicine and Biology, 2012, 57, 2329-2346.	1.6	106

#	Article	IF	CITATIONS
19	In Vivo Determination of Hepatic Stiffness Using Steady-State Free Precession Magnetic Resonance Elastography. Investigative Radiology, 2006, 41, 841-848.	3.5	105
20	How tissue fluidity influences brain tumor progression. Proceedings of the National Academy of Sciences of the United States of America, 2020, 117, 128-134.	3.3	103
21	MR elastography of the human heart: Noninvasive assessment of myocardial elasticity changes by shear wave amplitude variations. Magnetic Resonance in Medicine, 2009, 61, 668-677.	1.9	101
22	Magnetic resonance elastography reveals altered brain viscoelasticity in experimental autoimmune encephalomyelitis. NeuroImage: Clinical, 2012, 1, 81-90.	1.4	99
23	Alteration of brain viscoelasticity after shunt treatment in normal pressure hydrocephalus. Neuroradiology, 2012, 54, 189-196.	1.1	99
24	Viscoelastic properties of liver measured by oscillatory rheometry and multifrequency magnetic resonance elastography. Biorheology, 2010, 47, 133-141.	1.2	88
25	High-resolution mechanical imaging of the human brain by three-dimensional multifrequency magnetic resonance elastography at 7T. NeuroImage, 2014, 90, 308-314.	2.1	77
26	Cerebral magnetic resonance elastography in supranuclear palsy and idiopathic Parkinson's disease. NeuroImage: Clinical, 2013, 3, 381-387.	1.4	76
27	Wide-range dynamic magnetic resonance elastography. Journal of Biomechanics, 2011, 44, 1380-1386.	0.9	75
28	In vivo measurement of volumetric strain in the human brain induced by arterial pulsation and harmonic waves. Magnetic Resonance in Medicine, 2013, 70, 671-683.	1.9	73
29	InÂVivo Time Harmonic Elastography of the Human Heart. Ultrasound in Medicine and Biology, 2012, 38, 214-222.	0.7	72
30	In vivo wideband multifrequency MR elastography of the human brain and liver. Magnetic Resonance in Medicine, 2016, 76, 1116-1126.	1.9	70
31	Combining viscoelasticity, diffusivity and volume of the hippocampus for the diagnosis of Alzheimer's disease based on magnetic resonance imaging. NeuroImage: Clinical, 2018, 18, 485-493.	1.4	69
32	Tomoelastography of the abdomen: Tissue mechanical properties of the liver, spleen, kidney, and pancreas from single <scp>MR</scp> elastography scans at different hydration states. Magnetic Resonance in Medicine, 2017, 78, 976-983.	1.9	67
33	Analysis of wave patterns in MR elastography of skeletal muscle using coupled harmonic oscillator simulations. Magnetic Resonance Imaging, 2002, 20, 95-104.	1.0	66
34	Isovolumetric Elasticity Alteration in the Human Heart Detected by InÂVivo Time-Harmonic Elastography. Ultrasound in Medicine and Biology, 2013, 39, 2272-2278.	0.7	64
35	MR elastography in a murine stroke model reveals correlation of macroscopic viscoelastic properties of the brain with neuronal density. NMR in Biomedicine, 2013, 26, 1534-1539.	1.6	62
36	Collagen networks determine viscoelastic properties of connective tissues yet do not hinder diffusion of the aqueous solvent. Soft Matter, 2019, 15, 3055-3064.	1.2	60

#	Article	IF	CITATIONS
37	Scatter-based magnetic resonance elastography. Physics in Medicine and Biology, 2009, 54, 2229-2241.	1.6	58
38	In vivo waveguide elastography: Effects of neurodegeneration in patients with amyotrophic lateral sclerosis. Magnetic Resonance in Medicine, 2014, 72, 1755-1761.	1.9	58
39	In Vivo Abdominal Magnetic Resonance Elastography for the Assessment of Portal Hypertension Before and After Transjugular Intrahepatic Portosystemic Shunt Implantation. Investigative Radiology, 2015, 50, 347-351.	3.5	58
40	Tomoelastography Distinguishes Noninvasively between Benign and Malignant Liver Lesions. Cancer Research, 2019, 79, 5704-5710.	0.4	58
41	Fractal network dimension and viscoelastic powerlaw behavior: I. A modeling approach based on a coarse-graining procedure combined with shear oscillatory rheometry. Physics in Medicine and Biology, 2012, 57, 4023-4040.	1.6	57
42	Brain maturation is associated with increasing tissue stiffness and decreasing tissue fluidity. Acta Biomaterialia, 2019, 99, 433-442.	4.1	55
43	Tissue structure and inflammatory processes shape viscoelastic properties of the mouse brain. NMR in Biomedicine, 2015, 28, 831-839.	1.6	53
44	Cardiac MR Elastography: Comparison with left ventricular pressure measurement. Journal of Cardiovascular Magnetic Resonance, 2009, 11, 44.	1.6	51
45	Simulation and analysis of magnetic resonance elastography wave images using coupled harmonic oscillators and Gaussian local frequency estimation. Magnetic Resonance Imaging, 2001, 19, 703-713.	1.0	50
46	Threeâ€parameter shear wave inversion in MR elastography of incompressible transverse isotropic media: Application to in vivo lower leg muscles. Magnetic Resonance in Medicine, 2016, 75, 1537-1545.	1.9	47
47	Higherâ€resolution MR elastography reveals early mechanical signatures of neuroinflammation in patients with clinically isolated syndrome. Journal of Magnetic Resonance Imaging, 2016, 44, 51-58.	1.9	47
48	Two-dimensional waveform analysis in MR elastography of skeletal muscles. Physics in Medicine and Biology, 2005, 50, 1313-1325.	1.6	46
49	Nonlinear multiscale regularisation in MR elastography: Towards fine feature mapping. Medical Image Analysis, 2017, 35, 133-145.	7.0	46
50	Multifrequency Magnetic Resonance Elastography for the Assessment of Renal Allograft Function. Investigative Radiology, 2016, 51, 591-595.	3.5	44
51	Perfusion alters stiffness of deep gray matter. Journal of Cerebral Blood Flow and Metabolism, 2018, 38, 116-125.	2.4	44
52	Scattered Brain Infarct Pattern on Diffusion-Weighted Magnetic Resonance Imaging in Patients with Acute Ischemic Stroke. Cerebrovascular Diseases, 2001, 11, 157-163.	0.8	42
53	Cardiac Magnetic Resonance Elastography. Investigative Radiology, 2008, 43, 762-772.	3.5	42
54	Cardiac Magnetic Resonance Elastography. Investigative Radiology, 2010, 45, 782-787.	3.5	41

#	Article	IF	CITATIONS
55	Wideband MRE and static mechanical indentation of human liver specimen: Sensitivity of viscoelastic constants to the alteration of tissue structure in hepatic fibrosis. Journal of Biomechanics, 2014, 47, 1665-1674.	0.9	41
56	In vivo high-resolution magnetic resonance elastography of the uterine corpus and cervix. European Radiology, 2014, 24, 3025-3033.	2.3	40
57	Multifrequency Time-Harmonic Elastography for the Measurement of Liver Viscoelasticity in Large Tissue Windows. Ultrasound in Medicine and Biology, 2015, 41, 724-733.	0.7	40
58	Physical Function and Spinal Mobility Remain Stable Despite Radiographic Spinal Progression in Patients with Ankylosing Spondylitis Treated with TNF-α Inhibitors for Up to 10 Years. Journal of Rheumatology, 2016, 43, 2142-2148.	1.0	38
59	US Time-Harmonic Elastography: Detection of Liver Fibrosis in Adolescents with Extreme Obesity with Nonalcoholic Fatty Liver Disease. Radiology, 2018, 288, 99-106.	3.6	38
60	In vivo magnetic resonance elastography of human brain at 7 T and 1.5 T. Journal of Magnetic Resonance Imaging, 2010, 32, 577-583.	1.9	37
61	Shear-wave Amplitudes Measured with Cardiac MR Elastography for Diagnosis of Diastolic Dysfunction. Radiology, 2014, 271, 681-687.	3.6	37
62	<i>In vivo</i> time-harmonic multifrequency elastography of the human liver. Physics in Medicine and Biology, 2014, 59, 1641-1654.	1.6	35
63	A compact 0.5 T MR elastography device and its application for studying viscoelasticity changes in biological tissues during progressive formalin fixation. Magnetic Resonance in Medicine, 2018, 79, 470-478.	1.9	35
64	Towards compressionâ€sensitive magnetic resonance elastography of the liver: Sensitivity of harmonic volumetric strain to portal hypertension. Journal of Magnetic Resonance Imaging, 2014, 39, 298-306.	1.9	34
65	Serum C-reactive Protein Levels Demonstrate Predictive Value for Radiographic and Magnetic Resonance Imaging Outcomes in Patients with Active Ankylosing Spondylitis Treated with Golimumab. Journal of Rheumatology, 2016, 43, 1704-1712.	1.0	34
66	Two-Dimensional Time-Harmonic Elastography of the Human Liver and Spleen. Ultrasound in Medicine and Biology, 2016, 42, 2562-2571.	0.7	34
67	Tomoelastography of the prostate using multifrequency MR elastography and externally placed pressurizedâ€air drivers. Magnetic Resonance in Medicine, 2018, 79, 1325-1333.	1.9	34
68	Fast tomoelastography of the mouse brain by multifrequency singleâ€shot MR elastography. Magnetic Resonance in Medicine, 2019, 81, 2676-2687.	1.9	34
69	Increasing the spatial resolution and sensitivity of magnetic resonance elastography by correcting for subject motion and susceptibility-induced image distortions. Journal of Magnetic Resonance Imaging, 2017, 46, 134-141.	1.9	32
70	Time Harmonic Elastography Reveals Sensitivity of Liver Stiffness to Water Ingestion. Ultrasound in Medicine and Biology, 2016, 42, 1289-1294.	0.7	31
71	Progressive supranuclear palsy and idiopathic Parkinson's disease are associated with local reduction of in vivo brain viscoelasticity. European Radiology, 2018, 28, 3347-3354.	2.3	31
72	Multiparametric Quantitative MRI for the Detection of IgA Nephropathy Using Tomoelastography, DWI, and BOLD Imaging. Investigative Radiology, 2019, 54, 669-674.	3.5	31

#	Article	IF	CITATIONS
73	Elasticity-based determination of isovolumetric phases in the human heart. Journal of Cardiovascular Magnetic Resonance, 2010, 12, 60.	1.6	30
74	Heterogeneous Multifrequency Direct Inversion (HMDI) for magnetic resonance elastography with application to a clinical brain exam. Medical Image Analysis, 2018, 46, 180-188.	7.0	29
75	Tomoelastography of the native kidney: Regional variation and physiological effects on in vivo renal stiffness. Magnetic Resonance in Medicine, 2018, 79, 2126-2134.	1.9	28
76	Tomoelastography for the Evaluation of Pediatric Nonalcoholic Fatty Liver Disease. Investigative Radiology, 2019, 54, 198-203.	3.5	28
77	Hypercapnia increases brain viscoelasticity. Journal of Cerebral Blood Flow and Metabolism, 2019, 39, 2445-2455.	2.4	28
78	High-resolution mechanical imaging of the kidney. Journal of Biomechanics, 2014, 47, 639-644.	0.9	27
79	Measurement of in vivo cerebral volumetric strain induced by the Valsalva maneuver. Journal of Biomechanics, 2014, 47, 1652-1657.	0.9	26
80	Diagnostic performance of tomoelastography of the liver and spleen for staging hepatic fibrosis. European Radiology, 2020, 30, 1719-1729.	2.3	26
81	Biomechanical properties of the hypoxic and dying brain quantified by magnetic resonance elastography. Acta Biomaterialia, 2020, 101, 395-402.	4.1	26
82	In Vivo Quantification of Water Diffusion, Stiffness, and Tissue Fluidity in Benign Prostatic Hyperplasia and Prostate Cancer. Investigative Radiology, 2020, 55, 524-530.	3.5	26
83	Tabletop magnetic resonance elastography for the measurement of viscoelastic parameters of small tissue samples. Journal of Magnetic Resonance, 2015, 251, 13-18.	1.2	25
84	In vivo time-harmonic ultrasound elastography of the human brain detects acute cerebral stiffness changes induced by intracranial pressure variations. Scientific Reports, 2018, 8, 17888.	1.6	25
85	Tomoelastography Paired With T2* Magnetic Resonance Imaging Detects Lupus Nephritis With Normal Renal Function. Investigative Radiology, 2019, 54, 89-97.	3.5	25
86	Comparison of non-invasive assessment of liver fibrosis in patients with alpha1-antitrypsin deficiency using magnetic resonance elastography (MRE), acoustic radiation force impulse (ARFI) Quantification, and 2D-shear wave elastography (2D-SWE). PLoS ONE, 2018, 13, e0196486.	1.1	24
87	Reduction of breathing artifacts in multifrequency magnetic resonance elastography of the abdomen. Magnetic Resonance in Medicine, 2021, 85, 1962-1973.	1.9	24
88	Physiologic Reduction of Hepatic Venous Blood Flow by the Valsalva Maneuver Decreases Liver Stiffness. Journal of Ultrasound in Medicine, 2017, 36, 1305-1311.	0.8	21
89	Realâ€time MR elastography for viscoelasticity quantification in skeletal muscle during dynamic exercises. Magnetic Resonance in Medicine, 2020, 84, 103-114.	1.9	21
90	Cerebral multifrequency MR elastography by remote excitation of intracranial shear waves. NMR in Biomedicine, 2015, 28, 1426-1432.	1.6	20

#	Article	IF	CITATIONS
91	In vivo multifrequency magnetic resonance elastography of the human intervertebral disk. Magnetic Resonance in Medicine, 2015, 74, 1380-1387.	1.9	20
92	Measurement of vibrationâ€induced volumetric strain in the human lung. Magnetic Resonance in Medicine, 2013, 69, 667-674.	1.9	18
93	Cardiac-gated steady-state multifrequency magnetic resonance elastography of the brain: Effect of cerebral arterial pulsation on brain viscoelasticity. Journal of Cerebral Blood Flow and Metabolism, 2020, 40, 991-1001.	2.4	18
94	Tomoelastography for Measurement of Tumor Volume Related to Tissue Stiffness in Pancreatic Ductal Adenocarcinomas. Investigative Radiology, 2020, 55, 769-774.	3.5	18
95	Multifrequency magnetic resonance elastography of the brain reveals tissue degeneration in neuromyelitis optica spectrum disorder. European Radiology, 2017, 27, 2206-2215.	2.3	16
96	Magnetic resonance elastography quantification of the solid-to-fluid transition of liver tissue due to decellularization. Journal of the Mechanical Behavior of Biomedical Materials, 2020, 104, 103640.	1.5	16
97	Superviscous properties of the in vivo brain at large scales. Acta Biomaterialia, 2021, 121, 393-404.	4.1	16
98	US Time-Harmonic Elastography for the Early Detection of Glomerulonephritis. Radiology, 2019, 292, 676-684.	3.6	15
99	Time-Resolved Response of Cerebral Stiffness to Hypercapnia in Humans. Ultrasound in Medicine and Biology, 2020, 46, 936-943.	0.7	15
100	Phase preparation in steady-state free precession MR elastography. Magnetic Resonance Imaging, 2008, 26, 228-235.	1.0	14
101	Full-Field-of-View Time-Harmonic Elastography of the Native Kidney. Ultrasound in Medicine and Biology, 2018, 44, 949-954.	0.7	14
102	Fast Robust Dejitter and Interslice Discontinuity Removal in MRI Phase Acquisitions: Application to Magnetic Resonance Elastography. IEEE Transactions on Medical Imaging, 2019, 38, 1578-1587.	5.4	14
103	Ultrasound Time-Harmonic Elastography of the Aorta. Investigative Radiology, 2019, 54, 675-680.	3.5	14
104	Real-Time Multifrequency MR Elastography of the Human Brain Reveals Rapid Changes in Viscoelasticity in Response to the Valsalva Maneuver. Frontiers in Bioengineering and Biotechnology, 2021, 9, 666456.	2.0	14
105	Influence of fibrosis progression on the viscous properties of in vivo liver tissue elucidated by shear wave dispersion in multifrequency MR elastography. Journal of the Mechanical Behavior of Biomedical Materials, 2021, 121, 104645.	1.5	14
106	Liquid-Liver Phantom. Investigative Radiology, 2022, 57, 502-509.	3.5	14
107	Vibrationâ€synchronized magnetic resonance imaging for the detection of myocardial elasticity changes. Magnetic Resonance in Medicine, 2012, 67, 919-924.	1.9	13
108	Serum Vascular Endothelial Growth Factor Levels Lack Predictive Value in Patients with Active Ankylosing Spondylitis Treated with Golimumab. Journal of Rheumatology, 2016, 43, 901-906.	1.0	13

#	Article	IF	CITATIONS
109	The influence of body temperature on tissue stiffness, blood perfusion, and water diffusion in the mouse brain. Acta Biomaterialia, 2019, 96, 412-420.	4.1	13
110	Separation of fluid and solid shear wave fields and quantification of coupling density by magnetic resonance poroelastography. Magnetic Resonance in Medicine, 2021, 85, 1655-1668.	1.9	13
111	How histopathologic changes in pediatric nonalcoholic fatty liver disease influence in vivo liver stiffness. Acta Biomaterialia, 2021, 123, 178-186.	4.1	13
112	Feasibility of Intestinal <scp>MR</scp> Elastography in Inflammatory Bowel Disease. Journal of Magnetic Resonance Imaging, 2022, 55, 815-822.	1.9	13
113	Adipose cells and tissues soften with lipid accumulation while in diabetes adipose tissue stiffens. Scientific Reports, 2022, 12, .	1.6	13
114	Time-Harmonic Elastography of the Liver is Sensitive to Intrahepatic Pressure Gradient and Liver Decompression after Transjugular Intrahepatic Portosystemic Shunt (TIPS) Implantation. Ultrasound in Medicine and Biology, 2017, 43, 595-600.	0.7	11
115	Comparison of inversion methods in <scp>MR</scp> elastography: An openâ€access pipeline for processing multifrequency shearâ€wave data and demonstration in a phantom, human kidneys, and brain. Magnetic Resonance in Medicine, 2022, 88, 1840-1850.	1.9	11
116	Sensitivity of multifrequency magnetic resonance elastography and diffusion-weighted imaging to cellular and stromal integrity of liver tissue. Journal of Biomechanics, 2019, 88, 201-208.	0.9	9
117	Viscoelasticity of striatal brain areas reflects variations in body mass index of lean to overweight male adults. Brain Imaging and Behavior, 2020, 14, 2477-2487.	1.1	9
118	Ultrasound Time-Harmonic Elastography of the Pancreas. Investigative Radiology, 2020, 55, 270-276.	3.5	9
119	In vivo stiffness of multiple sclerosis lesions is similar to that of normal-appearing white matter. Acta Biomaterialia, 2022, 138, 410-421.	4.1	9
120	Time-Resolved Analysis of Left Ventricular Shear Wave Amplitudes in Cardiac Elastography for the Diagnosis of Diastolic Dysfunction. Investigative Radiology, 2016, 51, 1-6.	3.5	8
121	Time-Harmonic Ultrasound elastography of the Descending Abdominal Aorta: Initial Results. Ultrasound in Medicine and Biology, 2017, 43, 2550-2557.	0.7	8
122	Quantification of Aortic Stiffness by Ultrasound Time-Harmonic Elastography. Investigative Radiology, 2020, 55, 174-180.	3.5	8
123	Spatial heterogeneity of hepatic fibrosis in primary sclerosing cholangitis vs. viral hepatitis assessed by MR elastography. Scientific Reports, 2021, 11, 9820.	1.6	8
124	Added Value of Tomoelastography for Characterization of Pancreatic Neuroendocrine Tumor Aggressiveness Based on Stiffness. Cancers, 2021, 13, 5185.	1.7	8
125	Alterations of the proton-T2 time in relaxed skeletal muscle induced by passive extremity flexions. Journal of Magnetic Resonance Imaging, 2006, 23, 541-546.	1.9	7
126	Inversionâ€recovery MR elastography of the human brain for improved stiffness quantification near fluid–solid boundaries. Magnetic Resonance in Medicine, 2021, 86, 2552-2561.	1.9	7

#	Article	IF	CITATIONS
127	Microscopic multifrequency MR elastography for mapping viscoelasticity in zebrafish. Magnetic Resonance in Medicine, 2022, 87, 1435-1445.	1.9	7
128	Disease Activity Cutoff Values in Initiating Tumor Necrosis Factor Inhibitor Therapy in Ankylosing Spondylitis: A German GO-NICE Study Subanalysis. Journal of Rheumatology, 2020, 47, 35-41.	1.0	6
129	Changes in Liver Mechanical Properties and Water Diffusivity During Normal Pregnancy Are Driven by Cellular Hypertrophy. Frontiers in Physiology, 2020, 11, 605205.	1.3	6
130	Transtemporal Investigation of Brain Parenchyma Elasticity Using 2-D Shear Wave Elastography: Trustworthy?. Ultrasound in Medicine and Biology, 2019, 45, 1344-1345.	0.7	5
131	Tomoelastography for Longitudinal Monitoring of Viscoelasticity Changes in the Liver and in Renal Allografts after Direct-Acting Antiviral Treatment in 15 Kidney Transplant Recipients with Chronic HCV Infection. Journal of Clinical Medicine, 2021, 10, 510.	1.0	5
132	Noninvasive Detection of Intracranial Hypertension by Novel Ultrasound Time-Harmonic Elastography. Investigative Radiology, 2022, 57, 77-84.	3.5	5
133	Cerebral Ultrasound Time-Harmonic Elastography Reveals Softening of the Human Brain Due to Dehydration. Frontiers in Physiology, 2020, 11, 616984.	1.3	5
134	Steady-State Multifrequency Magnetic Resonance Elastography of the Thoracic and Abdominal Human Aorta—Validation and Reference Values. Investigative Radiology, 2020, Publish Ahead of Print, 451-456.	3.5	4
135	Effect of Post-mortem Interval and Perfusion on the Biophysical Properties of ex vivo Liver Tissue Investigated Longitudinally by MRE and DWI. Frontiers in Physiology, 2021, 12, 696304.	1.3	4
136	Solid fraction determines stiffness and viscosity in decellularized pancreatic tissues. , 2022, , 212999.		3
137	Higher-resolution MR elastography reveals early mechanical signatures of neuroinflammation in patients with clinically isolated syndrome. Journal of Magnetic Resonance Imaging, 2016, 44, spcone-spcone.	1.9	2
138	Tomoelastography by Multifrequency Wave Number Recovery. Informatik Aktuell, 2016, , 3-7.	0.4	2
139	Sensitivity of Tissue Shear Stiffness to Pressure and Perfusion in Health and Disease. , 2018, , 429-449.		2
140	Microscopic multifrequency magnetic resonance elastography of ex vivo abdominal aortic aneurysms for extracellular matrix imaging in a mouse model. Acta Biomaterialia, 2021, 140, 389-389.	4.1	2
141	Multifrequency magnetic resonance elastography-based tomoelastography of the parotid glands–feasibility and reference values. Dentomaxillofacial Radiology, 2022, 51, 20210337.	1.3	1
142	Shear Wave Diffusion Observed by Magnetic Resonance Elastography. Mathematics and Visualization, 2012, , 157-168.	0.4	1
143	In vivo time harmonic multiple frequency elastography of human liver. , 2012, , .		0
144	Fast 3D Vector Field Multi-Frequency Magnetic Resonance Elastography of the Human Brain. Informatik Aktuell, 2012, , 363-368.	0.4	0

#	Article	IF	CITATIONS
145	Direct Magnetic Resonance Elastography. Informatik Aktuell, 2012, , 3-8.	0.4	Ο
146	B-Mode-gestützte zeitharmonische Leber-Elastographie zur Diagnose hepatischer Fibrose bei adipösen Patienten. Informatik Aktuell, 2015, , 41-46.	0.4	0